

On the Photoreduction of Uranyl Complexes with Alkylphosphates in Nonaqueous Media

G. CAUZZO, G. GENNARI, G. GIACOMETTI, G. C. AGOSTINI and A. GAMBARO

Istituto Chimica Fisica dell'Università, Padua, Italy

Received May 18, 1978

Uranyl complexes with triethylphosphate and trimethylphosphate dissolved in the corresponding alkyl phosphates are photoreduced by irradiation in their UV–VIS absorption band. The photoreaction proceeds through the formation of an intermediate species which was identified as U(V). The latter is quite stable in the dark, but undergoes a photochemical disproportionation giving U(IV) as the final product.

Introduction

The fact that UO_2^+ is an intermediate in the photochemical reactions of UO_2^{2+} ion is generally accepted and there is also good indirect evidence of its formation in the process of quenching of uranyl luminescence by metal ions via electron transfer mechanism [1].

More direct evidence about this U(V) species is however quite difficult to obtain owing to its thermodynamic instability with respect to disproportionation to U(IV) and U(VI) [2].

Moreover, water is not a reagent for uranyl photoreduction [3] so that substrates such as alcohols, carbohydrates or carboxylic acids must be used in order to follow the photochemical reaction [4, 5].

On the other hand, the photochemistry of uranyl compounds in completely anhydrous media has been largely neglected and it seemed to us worthwhile to fill this gap and at the same time to look for a simplified situation where the solvent medium was playing the two simultaneous roles of complexant of the ion and also of photoreducing reagent. An ideal medium meeting these requirements is provided by trialkylphosphate esters, the well known extractants in the chemical processing of neutron irradiated uranium. Some qualitative photochemical interest in this medium has already been shown [6–9].

In this paper we report the results of our investigation on the photoreduction of the uranyl nitrate–triethyl phosphate complex, $\text{UO}_2(\text{NO}_3)_2 \cdot 2\text{TEP}$ (TEP = triethylphosphate). Triethylphosphate was also used as the solvent. Some data on the photo-

reduction of $\text{UO}_2(\text{NO}_3)_2 \cdot 2\text{TMP}$ (TMP = trimethylphosphate) dissolved in TMP are also reported.

The point of major interest of our findings arises from the fact that the experimental situation described allows a most precise determination of the role of the U(V) intermediate which, in this completely anhydrous medium, behaves under disproportionation in a quite different way from that which is found in the presence of water. In fact, we find that UO_2^+ is also photoreactive, and this opens new possible paths to the clarification of important aspects of uranyl photochemistry.

Experimental

Materials

Uranyl nitrate hexahydrate (Fluka *puriss.*) and uranium tetrachloride (Alfa product) were used without purification.

$\text{UO}_2(\text{NO}_3)_2 \cdot 2\text{TEP}$ (m.p. 80–85 °C) and $\text{UO}_2(\text{NO}_3)_2 \cdot 2\text{TMP}$ (m.p. 130–133 °C) were prepared by the procedure described by Bullock [10]. Purification was accomplished by several recrystallization from chloroform.

Purity of all solvents used was checked by vapour phase chromatography.

Spectra

Absorption spectra were determined by a Cary 14 and a Perkin-Elmer 139 spectrophotometers. Fluorescence measurements were carried out with a Perkin-Elmer MPF 44 spectrophotofluorimeter. The fluorescence quantum yields (ϕ_F) were determined by comparison of the spectra with that of perylene in degassed cyclohexane ($\phi_F = 0.78$) [11]. The calculations were made using the Parker and Rees formula [12], which was corrected for the refractive index difference between the solvent examined and cyclohexane [13].

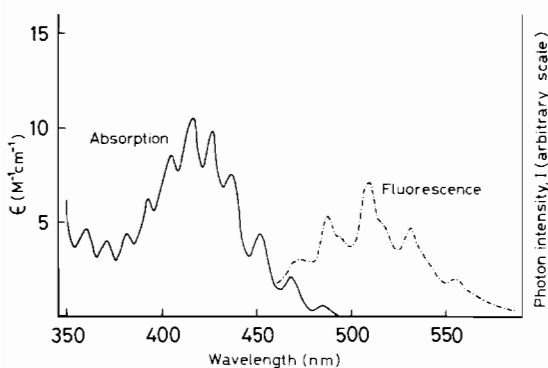
Magnetic Susceptibility Measurements

NMR measurements have been carried out at 298 K with a Bruker WH 90 spectrometer operating

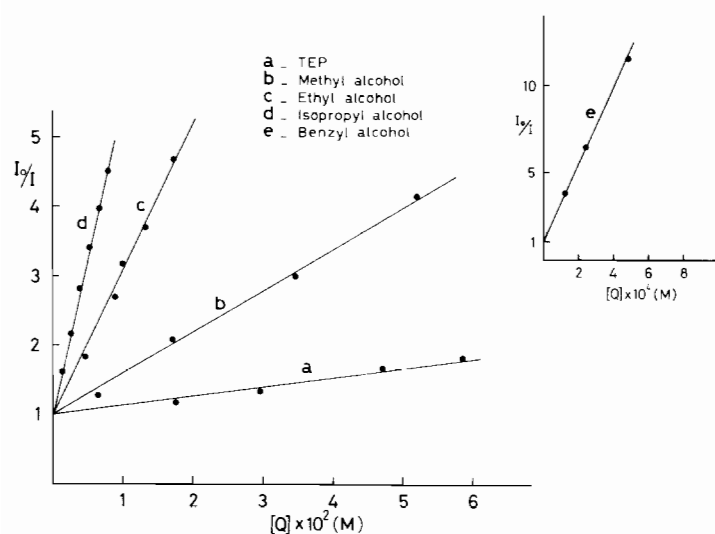
TABLE I. Fluorescence Quantum Yields (ϕ_F) of $\text{UO}_2(\text{NO}_3)_2 \cdot 2\text{TTEP}$ in Different Solvents.^a

Solvent	ϕ_F
TEP	3×10^{-4} ($\approx 6 \times 10^{-5}$)
CCl_4	6.1×10^{-3} (3.6×10^{-3})
CHCl_3	1×10^{-4}
CH_2Cl_2	4×10^{-4}
CH_3COCH_3	1.0×10^{-3}

^a $[\text{UO}_2(\text{NO}_3)_2 \cdot 2\text{TTEP}] = 1.0 \times 10^{-2} \text{ M}$, $\lambda_{\text{exc}} = 415 \text{ nm}$. The figures in parentheses refer to $[\text{UO}_2(\text{NO}_3)_2 \cdot 2\text{TTEP}] = 8.0 \times 10^{-2} \text{ M}$ and $\lambda_{\text{exc}} = 365 \text{ nm}$.

Figure 1. Absorption and fluorescence spectra of $\text{UO}_2(\text{NO}_3)_2 \cdot 2\text{TTEP}$ in TEP.

in FT mode. Magnetic susceptibility determinations were performed with the Evans method [14] using the benzene proton resonance as shift indicator. Benzene was added in small amounts to the solutions after irradiation.

Figure 2. Stern-Volmer plots for the quenching of $\text{UO}_2(\text{NO}_3)_2 \cdot 2\text{TTEP}$ fluorescence in CCl_4 by various organic compounds.TABLE II. Stern-Volmer Constants (K_{SV}) for the Quenching of $\text{UO}_2(\text{NO}_3)_2 \cdot 2\text{TTEP}$ Fluorescence in CCl_4 by Various Substrates. $\lambda_{\text{exc}} = 420 \text{ nm}$, $\lambda_{\text{em}} = 509 \text{ nm}$.

Quencher	$K_{\text{SV}} (\text{M}^{-1})$	$K_{\text{SV}} (\text{M}^{-1})^a$
TEP	13	
Methyl-OH	60	12
Ethyl-OH	210	62.5
Isopropyl-OH	450	113
Benzyl-OH	22,300	3200

^aReference 18.

Irradiation Procedure

A stabilized Osram HBO 500 W high pressure mercury lamp was used as the light source. The irradiation wavelength was selected by Balzer interference filters. Samples were placed in thermostatted Pyrex cells at $17 \pm 1^\circ \text{C}$. Oxygen was previously removed from the solutions by bubbling pure (UPP) nitrogen. For the determination of the photoreduction quantum yields, substrate concentrations and optical paths were chosen in order to have a total absorption of the incident light. A ferrioxalate actinometer was used to monitor the light intensity.

Results

Absorption and Fluorescence Measurements

The absorption and fluorescence spectra of $\text{UO}_2(\text{NO}_3)_2 \cdot 2\text{TTEP}$ dissolved in TEP are shown in Figure 1. The spectra are quite similar in other solvents such as CCl_4 , benzene (in this case, however, the fluorescence is undetectable), CHCl_3 , CH_2Cl_2 and acetone. The values of the fluorescence quantum yields, ϕ_F , in

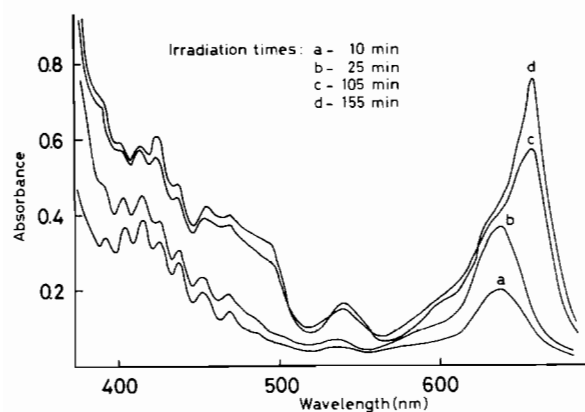


Figure 3. Changes in the absorption spectrum of $\text{UO}_2(\text{NO}_3)_2 \cdot 2\text{TEP}$ in TEP induced by the irradiation at 430 nm.

different solvents and at the same $\text{UO}_2(\text{NO}_3)_2 \cdot 2\text{TEP}$ concentration are given in Table I. Whereas the fluorescence spectra are the same when excited at different wavelengths in the visible and in the UV regions, the ϕ_F are concentration-dependent, as shown by the data in Table I. The quenching of $\text{UO}_2(\text{NO}_3)_2 \cdot 2\text{TEP}$ fluorescence in CCl_4 by various organic compounds is shown by the Stern–Volmer plots in Figure 2. The corresponding Stern–Volmer constants (K_{sv}) are reported in Table II.

Photoreduction Products

The changes in the absorption spectrum of deaerated $\text{UO}_2(\text{NO}_3)_2 \cdot 2\text{TEP}$ in TEP after irradiation at 430 nm are shown in Figure 3. A peak at 636 nm first appears, which is followed by a second one at 656 nm. The latter becomes dominant at very long irradiation times, and can be assigned to the final photoreduction product. Prolonged irradiation leads to the appearance of a gel, as previously found by Grdenic and Korpar [6] in the UO_2Cl_2 extracts with tributylphosphate. In the absence of oxygen both 636 and 656 nm peaks are very stable in the dark. In air saturated solutions, the absorptions slowly decrease, probably as a consequence of reoxidation processes, so that our experiments were carried out in an inert atmosphere (see Experimental).

By analogy with the results of previous photochemical experiments on uranyl complexes with alkylphosphates [6, 7] and from the resemblance of our final spectrum with that of the photoreduction product of uranyl in the presence of sucrose [8], we conclude that the absorption maximum at 656 nm belongs to U(IV), even if the products of ligand and/or solvent photooxidation have not been yet identified. The 636 nm peak has been tentatively assigned to U(V), the proposed intermediate in the photoreduction of U(VI) to U(IV) [4, 15]. We now see how this assignment is justified.

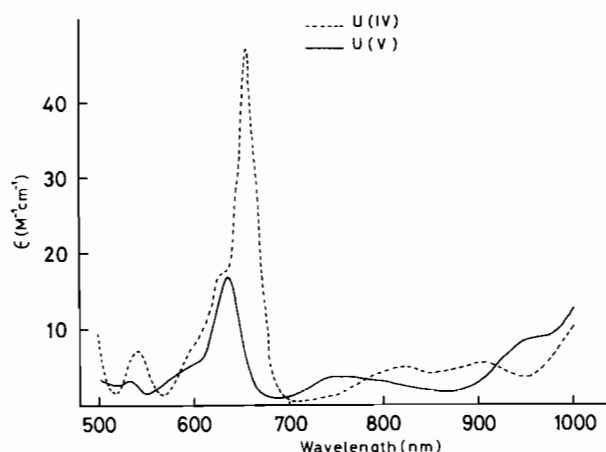


Figure 4. Absorption spectra of the U(V) and U(IV) species produced in the photoreduction of $\text{UO}_2(\text{NO}_3)_2 \cdot 2\text{TEP}$ in TEP.

By addition of 12M HCl to the irradiated TEP solutions (1:1 v/v), UCl_4 is produced, as shown by comparison with the absorption spectrum of pure UCl_4 in the same conditions ($\lambda_{\text{max}} = 670$ nm). The only other species observed was the unreduced uranyl. If the species with $\lambda_{\text{max}} = 636$ nm is identified as U(V), its conversion to UCl_4 is almost certainly due to a rapid acid catalyzed disproportionation, $2\text{U(V)} \rightarrow \text{U(VI)} + \text{U(IV)}$ [15]. The existence of this disproportionation is demonstrated by the following proof: irradiation of 1.20×10^{-4} mol of $\text{UO}_2(\text{NO}_3)_2 \cdot 2\text{TEP}$ in 6 cm³ of TEP for a suitable time produces an almost quantitative U(VI) \rightarrow U(V) conversion with the exclusion of U(IV), as demonstrated by the disappearance of the U(VI) peaks in the 350–500 nm region and by the formation of a single peak at 636 nm. After addition of HCl to this solution, 5.1×10^{-5} mol of UCl_4 were obtained, i.e., about half the original $\text{UO}_2(\text{NO}_3)_2 \cdot 2\text{TEP}$.

On the other hand, after a long irradiation of the TEP solution, only the final photoreduction product U(IV) is obtained, as shown by the constancy of its absorption spectrum ($\lambda_{\text{max}} = 656$ nm) for successive irradiations, until a gel is formed.

The spectra of U(V) and U(IV) species, as determined by the above procedure, are shown in Figure 4. These spectra were used for the spectrophotometric analysis of the irradiated solutions in the kinetic experiments (see later).

The spectral changes of the irradiated $\text{UO}_2(\text{NO}_3)_2 \cdot 2\text{TMP}$ in TMP are quite similar. In this case, however, the absorption due to U(V) is rather low and slowly vanishes in the dark. Therefore, our kinetic experiments were carried out on the $\text{UO}_2(\text{NO}_3)_2 \cdot 2\text{TEP}$ complex in TEP.

Magnetic Susceptibility Measurements

In order to confirm the attribution of the intermediate species and of the final product in the photo-

TABLE III. NMR Experiments on $\text{UO}_2(\text{NO}_3)_2 \cdot 2\text{TTEP}$ in TEP at 298 K.

Experiment	PS (H_2) ^a	$\delta_{\text{CH}_2}^i$ (H_2) ^b	$\delta_{\text{CH}_3}^i$ (H_2) ^b
$[\text{UO}_2(\text{NO}_3)_2 \cdot 2\text{TTEP}] = 0.696 \text{ M}$	—	284.6	541.2
$[\text{UO}_2(\text{NO}_3)_2 \cdot 2\text{TTEP}] = 0.549 \text{ M}$ [Intermediate species] = 0.129 M [Final product] = 0.018 M	59.0	265.3	538.5
$[\text{UO}_2(\text{NO}_3)_2 \cdot 2\text{TTEP}] = 0.522 \text{ M}$ [Intermediate species] = 0.019 M [Final product] = 0.155 M	93.6	284.6	541.2

^aUpfield paramagnetic shift of the internal benzene probe. ^bUpfield chemical shifts relative to benzene as internal standard.

reduction of uranyl nitrate complexes with alkyl-phosphates, the changes in the magnetic susceptibility produced by irradiation have been determined. Our experiments refer to the complex $\text{UO}_2(\text{NO}_3)_2 \cdot 2\text{TTEP}$ in TEP.

The irradiated solutions display a shift of the NMR spectrum as a whole towards high fields with respect to the original solutions indicating paramagnetic species production. In Table III are collected the results obtained with a 0.696 M solution of $\text{UO}_2(\text{NO}_3)_2 \cdot 2\text{TTEP}$ which was irradiated for suitable times in order to obtain an almost selective production of the intermediate species or of the final product, whose concentrations were determined from their optical spectra as previously described.

A glance at Table III shows that the proton spectra of the ligand are the same for the diamagnetic $\text{UO}_2(\text{NO}_3)_2 \cdot 2\text{TTEP}$ complex and for the final product, but a specific downfield shift is clearly displayed in the presence of the intermediate species (19.3 Hz for CH_2 and 2.7 Hz for CH_3 protons). In the latter case a broadening of the resonances is also observed, mainly for the CH_2 protons.

The molar paramagnetic shifts, calculated from the measured values in Table III, are 379.6 and 557.3 Hz for the intermediate specie and the final product, respectively. With these values we calculated the molar susceptibilities, using the simplified Evans relation [14]

$$\chi_M = \frac{3}{2\pi} \frac{\Delta M \times 10^{-3}}{\nu_0}$$

where ΔM is the molar paramagnetic shift and ν_0 is the instrument working frequency (in our case 90 MHz). In this way, we obtain $\chi_M = 2014 \times 10^{-6}$ for the intermediate species and $\chi_M = 2957 \times 10^{-6}$ for the final product. These values are to be compared with those calculated at 298 K for the iso-electronic species NpO_2^{2+} (1666×10^{-6}) and PuO_2^{2+} (3157×10^{-6}) ions, from accurate ESR data by

Eisenstein and Price [16, 17]. We feel that this is sufficient agreement to confirm the assignment of intermediate species in the photoreduction of $\text{UO}_2(\text{NO}_3)_2 \cdot 2\text{TTEP}$ as UO_2^+ and of the final product as UO_2 .

The differences in the calculated and experimental values are to be attributed on one side to the crudeness of our susceptibility determinations and on the other to the different crystal fields produced by the phosphate-nitrate complex of the experiment as compared to the crystal hosts of the ESR measurements.

Photoreduction of $\text{UO}_2(\text{NO}_3)_2 \cdot 2\text{TTEP}$ in Other Solvents

The photoreduction of $\text{UO}_2(\text{NO}_3)_2 \cdot 2\text{TTEP}$ takes place also in CCl_4 . In these conditions, however, a slight turbidity appears at the beginning of the photoreaction, which is followed at later irradiation times by the preccipitation of the photoproducts.

$\text{UO}_2(\text{NO}_3)_2 \cdot 2\text{TTEP}$ is not photoreduced in benzene. Benzene also strongly inhibits the photoreduction in CCl_4 and in TEP. This effect is consistent with the observed quenching of excited uranyl by aromatic hydrocarbons [18].

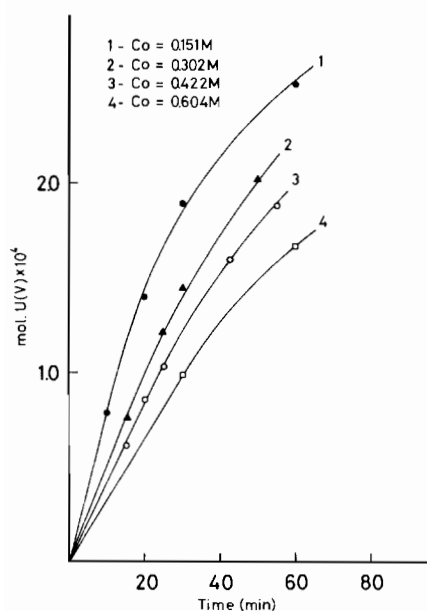
Kinetic Experiments

The amounts of the intermediate U(V) species produced in the photoreduction of $\text{UO}_2(\text{NO}_3)_2 \cdot 2\text{TTEP}$ in TEP are plotted in Figure 5 at various irradiation times and at different substrate concentrations. Since no appreciable formation of U(IV) takes place in the initial stages of the photoprocess, U(V) can be easily determined from its absorption at 636 nm.

As the absorption spectra of U(V) and $\text{UO}_2(\text{NO}_3)_2 \cdot 2\text{TTEP}$ overlap at the irradiation wavelength (430 nm), the quantum yields of U(V) formation, $\phi_{\text{U(V)}}$, were determined from the initial slopes of the plots. The values of $\phi_{\text{U(V)}}$ at different $\text{UO}_2(\text{NO}_3)_2 \cdot 2\text{TTEP}$ concentrations are reported in Table IV. The

TABLE IV. Quantum Yields of U(V) Formation, $\phi_{U(V)}$, at Different $UO_2(NO_3)_2 \cdot 2TEP$ Concentrations at 17 °C.

$[UO_2(NO_3)_2 \cdot 2TEP] (M)$	$\phi_{U(V)}$
0.151	0.25 ₁
0.304	0.16 ₀
0.422	0.13 ₃
0.604	0.10 ₁

Figure 5. Amounts of U(V) produced at various irradiation times in the photoreduction of $UO_2(NO_3)_2 \cdot 2TEP$ in TEP at different initial concentrations. Irradiation was at 430 nm; optical depths were chosen in order to achieve a total absorption of the incident light.

$\phi_{U(V)}$ were found to be independent of the light intensity and of the irradiation wavelength.

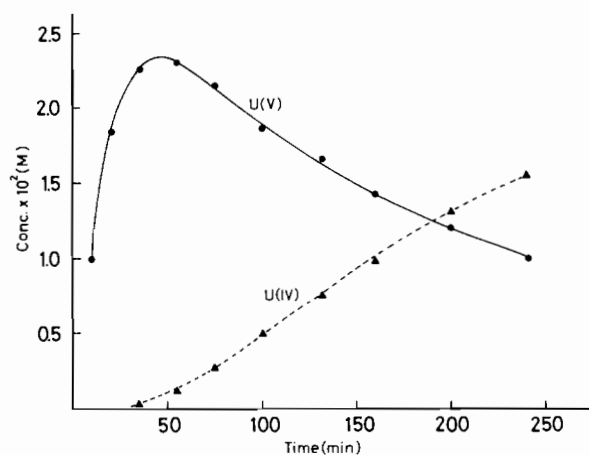
The progress of the photoreduction for larger conversion percentages was followed by the spectrophotometric analysis previously outlined. An example of the $[U(V)]$ and $[U(IV)]$ plots vs. irradiation time is shown in Figure 6. Similar curves were determined at different initial $UO_2(NO_3)_2 \cdot 2TEP$ concentrations, and the values of $[U(V)]$ and $[U(IV)]$ at the maxima of the $[U(V)]$ plots are reported in Table V.

Discussion

The uranyl complexes $UO_2(NO_3)_2 \cdot 2TEP$ and $UO_2(NO_3)_2 \cdot 2TMP$ dissolved in the corresponding alkylphosphates, undergo photoreduction giving uranium in the +4 oxidation state as the final product. The U(IV) formation has been recently also observed

TABLE V. Concentrations of U(V) and U(IV) (M), at the Maxima of the $[U(V)]$ vs. Time Plots at Different Initial $UO_2(NO_3)_2 \cdot 2TEP$ Concentrations, $[U(VI)]_0$, at 17 °C.

$[U(VI)]_0 \times 10^2$	$[U(V)]_m \times 10^2$	$[U(IV)]_m \times 10^3$
1.15	0.88	0.5
1.57	1.22	0.5
1.92	1.44	0.7
2.34	1.75	0.7
3.39	2.33	0.8
4.45	2.94	0.8
4.65	2.91	1.0
7.65	4.08	1.8
9.30	4.64	2.0
20.17	6.80	3.5

Figure 6. Plots of U(V) and U(IV) concentrations vs. irradiation time in the photoreduction of $3.39 \times 10^{-2} M UO_2(NO_3)_2 \cdot 2TEP$ in TEP. Irradiation at 430 nm.

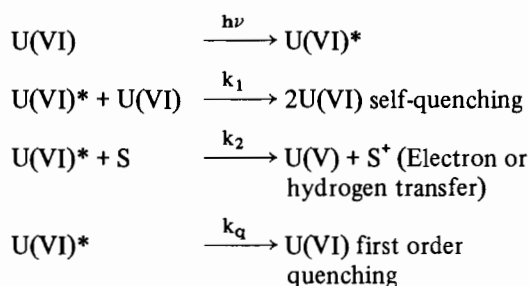
by Rofer de Poorter and de Poorter [9] in the photoreduction of uranyl nitrate in tributylphosphate.

The $UO_2(NO_3)_2 \cdot 2TEP$ complex is also photoreduced in an inert solvent such as CCl_4 . Although kinetic investigation in this solvent was not performed because of the low solubility of the photoreduction products, this observation may suggest a contribution of an intramolecular mechanism for the photoreduction of $UO_2(NO_3)_2 \cdot 2TEP$. The quenching of the excited uranyl by TEP ligands is also suggested by the low fluorescence intensity of $UO_2(NO_3)_2 \cdot 2TEP$ in CCl_4 (Table I).

The fluorescence of $UO_2(NO_3)_2 \cdot 2TEP$ in CCl_4 is quenched by several organic compounds. The Stern-Volmer plots are shown in Figure 2 and the corresponding Stern-Volmer constants, K_{sv} , are reported in Table II. In the same table the data of Matsushima [18] for UO_2^{2+} in water are also collected for comparison purposes. The parallelism of the two sets of data

strongly indicates the presence of the same quenching mechanism of the photoexcited uranyl in both cases.

The photoreduction of $\text{UO}_2(\text{NO}_3)_2 \cdot 2\text{TTEP}$ in TEP occurs *via* the formation of a thermally stable paramagnetic species which may be identified as UO_2^+ on the grounds of its acid-catalyzed disproportionation and magnetic properties. The observation of the U(V) intermediate in these conditions is very useful for a detailed kinetic investigation of the $\text{U(VI)} \rightarrow \text{U(IV)}$ photoreduction. As shown in Table IV, the quantum yield for the initial formation of U(V) decreases with increasing $\text{UO}_2(\text{NO}_3)_2 \cdot 2\text{TTEP}$ concentration. This observation can be explained by the self-quenching of the photoexcited uranyl [15] and the initial stage of the photoreduction, *i.e.* prior to the appearance of the U(IV) species, can be described by the following already proposed scheme:



The application of the steady state treatment for U(VI)* species leads to the following relation:

$$\frac{1}{\phi_{\text{U(V)}}} = 1 + \frac{k_q}{k_2} + \frac{k_1}{k_2} [\text{U(VI)}] \quad (1)$$

where $[\text{U(VI)}]$ is the initial $\text{UO}_2(\text{NO}_3)_2 \cdot 2\text{TTEP}$ concentration. Eq. (1) is illustrated by the plot in Figure 7. From the slope and the intercept one obtains $k_q/k_2 \approx 1$ and $k_1/k_2 \approx 13 \text{ M}^{-1}$, respectively.

The concentration dependence of $\phi_{\text{U(V)}}$ can be correlated with the observed self quenching of $\text{UO}_2(\text{NO}_3)_2 \cdot 2\text{TTEP}$ fluorescence. Even if a correlation between photoreduction and fluorescence quantum yields cannot be established from our data, it is reasonable to identify the fluorescent state with the photoexcited of U(VI)* species.

At the later stages of the photoreduction, detectable amounts of U(IV) begin to be formed, and the rise of its concentration is accompanied by a decrease in that of U(V), as shown in Figure 6. The shape of the U(IV) plot indicates that the whole photoprocess is a two-step consecutive reaction. Since the intermediate U(V) species is quite stable in the dark, U(IV) must be produced by reduction of the photoexcited U(V)* . As shown in Table V, in the more diluted solutions the maxima in the U(V) plots correspond to a higher photoreduction percentage. This observation indicates a photochemical bimolecular reaction of U(V), the more obvious being its disproportion to U(IV) and U(VI), $\text{U(V)*} +$

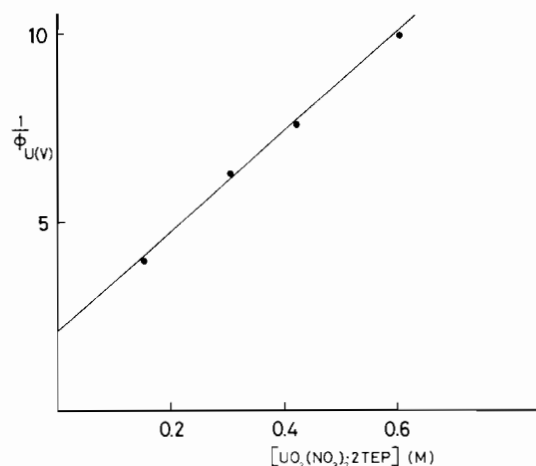
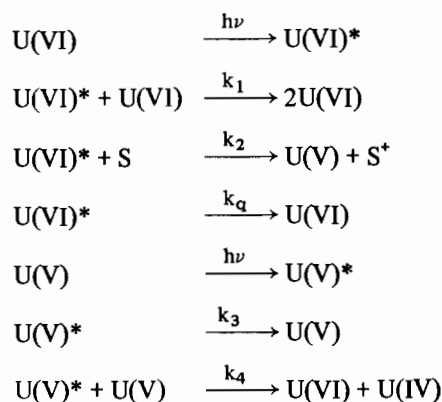


Figure 7. Plot of $1/\phi_{\text{U(V)}}$ vs. initial $\text{UO}_2(\text{NO}_3)_2 \cdot 2\text{TTEP}$ concentration in TEP.

$\text{U(V)} \rightarrow \text{U(IV)} + \text{U(VI)}$. The full mechanism of the $\text{UO}_2(\text{NO}_3)_2 \cdot 2\text{TTEP}$ photoreduction can be described thus:



Although the details of the $[\text{U(V)}]$ vs. time plots depend in a complicated fashion on the relative absorbance of the substrate and of its photoproducts at the irradiation wavelength, the heights of the maxima in the $[\text{U(V)}]$ can be easily correlated with the residual $\text{UO}_2(\text{NO}_3)_2 \cdot 2\text{TTEP}$ concentrations. If the steady state treatment is applied to the photoexcited U(VI)* and U(V)* species, together with the condition $d[\text{U(V)}]/dt = 0$ (for the U(V) maxima) the following relation is obtained from the above mechanism:

$$\frac{[\text{U(V)}]_m}{[\text{U(VI)}]_m} \left(1 + \frac{k_q}{k_2} + \frac{k_1}{k_2} [\text{U(VI)}]_m \right) = \frac{\epsilon_1}{\epsilon_2} \left(1 + \frac{k_3}{k_4 [\text{U(V)}]_m} \right) \quad (2)$$

where $[\text{U(V)}]_m$ and $[\text{U(VI)}]_m$ refer to the maxima of the U(V) plots; ϵ_1 and ϵ_2 are the U(V) and UO_2-

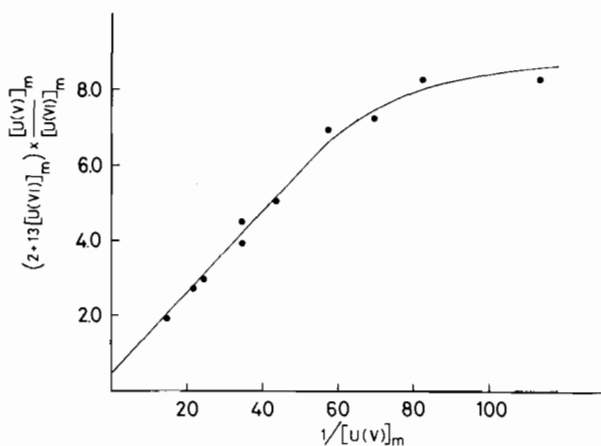


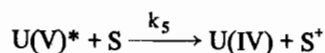
Figure 8. Plot of the data in Table V according to Eq. 3.

$(\text{NO}_3)_2 \cdot 2\text{TTEP}$ extinction coefficients at the irradiation wavelength (430 nm).

Inserting the values of $k_q/k_2 = 1$ and $k_1/k_2 = 13 M^{-1}$, Eq. (2) becomes

$$\frac{[\text{U(V)}]_m}{[\text{U(VI)}]_m} (2 + 13 [\text{U(VI)}]_m) = \frac{\epsilon_1}{\epsilon_2} \left(1 + \frac{k_3}{k_4 [\text{U(V)}]_m} \right) \quad (3)$$

In Figure 8, the values of the left-hand side of Eq. (3) are plotted vs. $1/[\text{U(V)}]_m$. The deviation from the linearity of the plot for the more diluted solutions may be ascribed to the existence of a direct reduction of the photoexcited U(V)^* by the solvent. Including the step



in the above mechanism one obtains

$$\frac{[\text{U(V)}]_m}{[\text{U(VI)}]_m} (2 + 13 [\text{U(VI)}]_m) = \frac{\epsilon_1}{\epsilon_2} \left(1 + \frac{k_3}{k_4 [\text{U(V)}]_m + k_5} \right) \quad (4)$$

This expression shows that appreciable deviations from Eq. (3) arise at low values of $[\text{U(V)}]_m$, when $k_4 [\text{U(V)}]_m$ becomes comparable to k_5 . The photoreduction of the U(V) intermediate may also explain the observed quantum yields in U(IV) (greater than 0.5) in the photoreduction of UO_2^{2+} in aqueous medium, as reported by Bell and Buxton [19].

Conclusions

The mechanism of the UO_2^{2+} photoreduction which we have put forward is of some interest also with

respect to the question of the chemical identity of the photoreduced uranium and of its redox properties. The two main findings are the stability of the U(V) species in the dark on one side and its photodisproportionation on the other.

The notion of a stable U(V) species in nonaqueous media was already established for the dimethylsulfoxide medium from electrochemical experiments by Gritzner and Selbin [20]. One might be tempted to compare the spectral data given by these authors and also some other scattered data on alleged UO_2^+ species in different media [21], particularly in the region above 1000 nm, in order to strengthen the assignment of the intermediate spectrum of Fig. 4 to UO_2^+ . We find, in fact, sharp features at 1085, 1300 and 1440 nm for our intermediate spectrum (not reported in the Figure) but we feel that the intensity and the position of these low energy bands (certainly originating from f-f Laporte forbidden transitions) are so strongly dependent on the symmetry and intensity of the ligand field that a comparison of spectra taken in so different media is meaningless.

Some speculations about the stability of U(V) in nonaqueous solution may be attempted by referring to what happens in water. In this latter medium, according to Kraus *et al.* [22], there is a small pH range of optimum stability between 2 and 4 due to a complex interplay of the hydrolytic behaviour of the UO_2^{2+} and UO_2^+ ions in connection with their rather close redox potentials in this pH range. In general, however, the detectability of U(V) in water, when possible, is due to the slowness of the hydrolytic reactions.

In the phosphate medium redox potentials are certainly affected and it may well be that the UO_2^+ ion is thermodynamically stable with respect to disproportionation.

It must be also emphasized that the phosphate medium may maintain some species in a metastable state, when these are produced *in situ* and this may explain the solubility of the final photoreduction product, which under these conditions may well exist in a complexed UO_2 form.

The important effect of the medium in changing the features of the photochemistry of this system is also apparent in the values of the rate constants involved. For instance, our calculated value of k_1/k_2 is approximately 13 while the same ratio in aqueous acidic solution is only about 3 [23].

Further flash photolytic and electrochemical studies on this system are needed in order to elucidate the thermodynamics and the kinetics of the two redox couples in this medium.

References

1. M. Moriyasu, Y. Yokoyama and S. Ikeda, *J. Inorg. Nucl. Chem.*, **39**, 2205 (1977) and references therein.
2. J. Selbin and J. D. Ortego, *Chem. Rev.*, **69**, 657 (1969).

- 3 M. Moriyasu, Y. Yokoyama and S. Ikeda, *J. Inorg. Nucl. Chem.*, **39**, 2211 (1977).
- 4 R. Matsushima and S. Sakuraba, *J. Am. Chem. Soc.*, **93**, 5421 (1971).
- 5 R. J. Hill, T. J. Kemp, D. M. Allen and A. Cox, *J. Chem. Soc. Faraday I*, **70**, 847 (1974).
- 6 D. Grdenic and B. Korpar, *J. Inorg. Nucl. Chem.*, **12**, 149 (1959).
- 7 A. S. Kertes and M. Halpern, *J. Inorg. Nucl. Chem.*, **19**, 359 (1961).
- 8 L. J. Heidt and K. A. Moon, *J. Am. Chem. Soc.*, **75**, 5803 (1953).
- 9 C. K. Rofer-de Poorter and G. L. de Poorter, *J. Inorg. Chem.*, **39**, 631 (1977).
- 10 J. I. Bullock, *J. Inorg. Nucl. Chem.*, **29**, 2257 (1967).
- 11 J. B. Birks, "Photophysics of Aromatic Molecules", Wiley-Interscience, London (1970) p. 123.
- 12 C. A. Parker and W. T. Rees, *Analyst*, **85**, 587 (1960).
- 13 J. B. Birks, "Photophysics of Aromatic Molecules", Wiley-Interscience London (1970) p. 98.
- 14 D. F. Evans, *J. Chem. Soc.*, 2003 (1959).
- 15 S. Sakuraba and R. Matsushima, *Bull. Chem. Soc. Japan*, **43**, 2359 (1970).
- 16 J. C. Eisenstein and M. H. L. Pryce, *Proc. Roy. Soc.*, **229**, 20 (1955).
- 17 J. C. Eisenstein and M. H. L. Pryce, *Proc. Roy. Soc.*, **238**, 31 (1957).
- 18 R. Matsushima, *J. Am. Chem. Soc.*, **94**, 6010 (1972).
- 19 J. T. Bell and S. R. Buxton, *J. Inorg. Nucl. Chem.*, **37**, 1469 (1975).
- 20 G. Gritzner and J. Selbin, *J. Inorg. Nucl. Chem.*, **30**, 1799 (1968).
- 21 D. A. Wenz, M. D. Adams, and R. K. Steunenberg, *Inorg. Chem.*, **3**, 989 (1964); D. Cohen, *J. Inorg. Nucl. Chem.*, **32**, 3525 (1970).
- 22 K. A. Kraus, F. Nelson and G. L. Johnson, *J. Am. Chem. Soc.*, **71**, 2510 (1949).
- 23 P. Benson, A. Cox, T. Kemp and Q. Sultana, *Chem. Phys. Letters*, **35**, 195 (1975).